

Two-Axial Gyroscope with Magnetically Supported Rotor

Zdzisław Gosiewski, Krzysztof Falkowski

Department of Armament and Aviation, Military University of Technology
ul. Kaliskiego 2, 01-489 Warsaw, POLAND
tel: +48(022)-685-67-19, e-mail: gosiewsk@zoial.wat.war.pl

Abstract: Gyroscope with magnetically suspended rotor is considered in the paper. There are used two models of gyroscope dynamics: full and simplified. The control law is designed for simplified linear instrument model. Controller consists of observer and LQR regulator. The same control law is joined to the full model and simplified one. To check performance of the gyroscope its dynamics and measurement path are simulated. The results of simulation can be useful for gyroscope designer.

1 Introduction

Almost each aircraft is equipped in independent from external sources (satellites, radio beacons) autonomous system of inertial navigation (INS). Such system produces information about spatial orientation, speed and localisation of the aircraft against the Earth. INS consists of accelerometers, gyroscopes, and navigational computer [4].

The accuracy of INS operation depends on the accuracy of the navigational instruments: accelerometers and gyroscopes and of the computer algorithms calculating localisation and spatial orientation of the aircraft. For example the drift of gyroscope should be below $0.1^\circ/\text{h}$ and measurement range up to $400^\circ/\text{s}$. The sensitivity of navigational instruments with mechanically supported inertial masses is limited by dry friction in kinematics pairs. Therefore gyroscopes with electrostatically supported rotors were used for space navigation. Such gyroscope is sensitive to small angular speed and linear accelerations but its measurement range is limited by available low electrostatic forces so it can not be used in gravitational field of Earth.

In this paper the gyroscope with magnetically suspended rotor is considered. In this case the physical contact of mechanical parts is also eliminated, what can increase the sensitivity of measurement. Magnetic forces are much higher than electrostatic ones therefore it is expected that such gyroscope will be properly operated in gravitational field of the Earth. From second hand the rotor freely levitates in magnetic field so its mass centre usually does not cover with centre of rotation. It causes that beside the gyrostatic moment there are additional moments of forces connected with translational motion which can introduce measurement errors. The influence of these moments will be studied.

Control laws for magnetic bearings are calculated for simplified linear model of rotor motion. The aircraft angular velocity is calculated from control and measurement signals [5]. To describe measurement error

the full and simplified models of rotor motion are derived. The known step signals of angular velocity and linear acceleration are put into simulated simplified and full models and into simulated measurement paths. The response signals are compared with input signals to calculate measurement errors. The simulation is conducted with assumptions that measurement has been ideal (without noise) and that bearings have got ideal characteristics.

2 Instrument

The rotor of the gyroscope in the form of full or empty cylinder is suspended in the magnetic field by set of electromagnets fixed to the instrument frame as it is shown in Fig. 1. Rotor is put into rotation (with constant angular speed Ω) by electric motor fixed in the middle of instrument. We take into consideration such instrument in which the axis

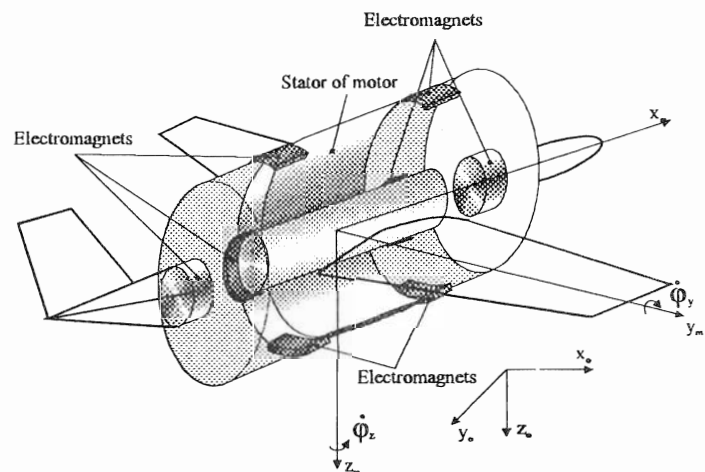


Fig. 1. Instrument orientation in the aircraft and co-ordinate systems.

of rotor rotation covers with longitudinal axis of the aircraft. Gyroscope is mechanically, magnetically and electrically symmetric in relation to its longitudinal axis and to the plane which crosses the centre of gravity and is perpendicular to the longitudinal axis. We introduce three right-hand co-ordinate systems.

1. Inertial system $O_0x_0y_0z_0$ in which the Newton laws are valid. For aircraft navigational purposes we can use the pseudoinertial co-ordinate system connected with Earth but which does not take part in her day and night motion. Centre O_0 is in the middle of Earth and axis z_0 is directed to South Pole.

- Co-ordinate system Oxyz is connected with aircraft frame. Point O is a geometric centre of the instrument case and the direction of Ox-axis is consistent with direction of longitudinal axis of the aircraft.
- Co-ordinate system $O_m x_m y_m z_m$ is rigidly connected with rotor. Point O_m covers with rotor mass centre and its axes cover with principal axes of inertia.

Rotor as a free body has six degree of freedom. Therefore, rotor motion is described by six co-ordinates:

x, y, z - linear co-ordinates which describes linear movement (translational motion) of rotor mass centre in Oxyz co-ordinate system,

γ, β, α - angular co-ordinates which describes angular movement (rotational motion) of the rotor around axes Ox, Oy, Oz, respectively.

Above co-ordinates can be collected into one vector of global co-ordinate system:

$$S_1 = [\gamma \quad x \quad \alpha \quad y \quad \beta \quad z]^T \quad (1)$$

The global co-ordinates can not be used directly. It is better to use local co-ordinates of the rotor motion in the magnetic bearing planes which form the vector of local co-ordinate system:

$$S_2 = [\gamma \quad x \quad y_l \quad y_p \quad z_l \quad z_p]^T \quad (2)$$

where: y_l, y_p - linear motion of the rotor in the direction of axis Oy in the left and in the right bearing planes, respectively,

z_l, z_p - linear motion of the rotor in the direction of axis Oz in the left and in the right bearing planes, respectively.

3 Translational motion

The measurement frame of references is the co-ordinate system Oxyz connected with aircraft. Translational relative motion of the rotor mass centre can be derived from Newtonian law:

$$m\bar{a} = \bar{F}_e + m\bar{g} - m(\bar{a}_u + \bar{a}_c) + \bar{F}_s, \quad (3)$$

where: m - rotor mass,
 a - relative acceleration,
 g - gravity acceleration,

$\bar{a}_u = \bar{a}_0 + \bar{\varepsilon} \times \bar{r} + \bar{\omega} \times (\bar{\omega} \times \bar{r})$ - acceleration of translation,

$\bar{a}_c = 2\bar{\omega} \times \bar{v}$ - Coriolis acceleration.

F_e - resultant force generated by electromagnets,

F_s - electromagnetic force generated by electric motor,

ω - angular velocity of aircraft,

a_0 - linear acceleration of the aircraft,

r - relative displacement of mass centre,

v - relative velocity of rotor mass centre,

ε - angular acceleration of the aircraft.

Above equation can be expanded into the set of three scalar equations in the Oxyz system:

$$\begin{aligned} m\ddot{x} &= F_{ex} + mg_x - m(\bar{a}_u + \bar{a}_c)_x, \\ m\ddot{y} &= F_{ey} + mg_y - m(\bar{a}_u + \bar{a}_c)_y + F_{sy}, \\ m\ddot{z} &= F_{ez} + mg_z - m(\bar{a}_u + \bar{a}_c)_z + F_{sz}, \end{aligned} \quad (4)$$

where: F_{ex} - force generated by axial electromagnets, $F_{ey} = F_{ly} + F_{py}$, $F_{ez} = F_{lz} + F_{pz}$ - forces generated by left and right radial electromagnets in the directions y and z, respectively.

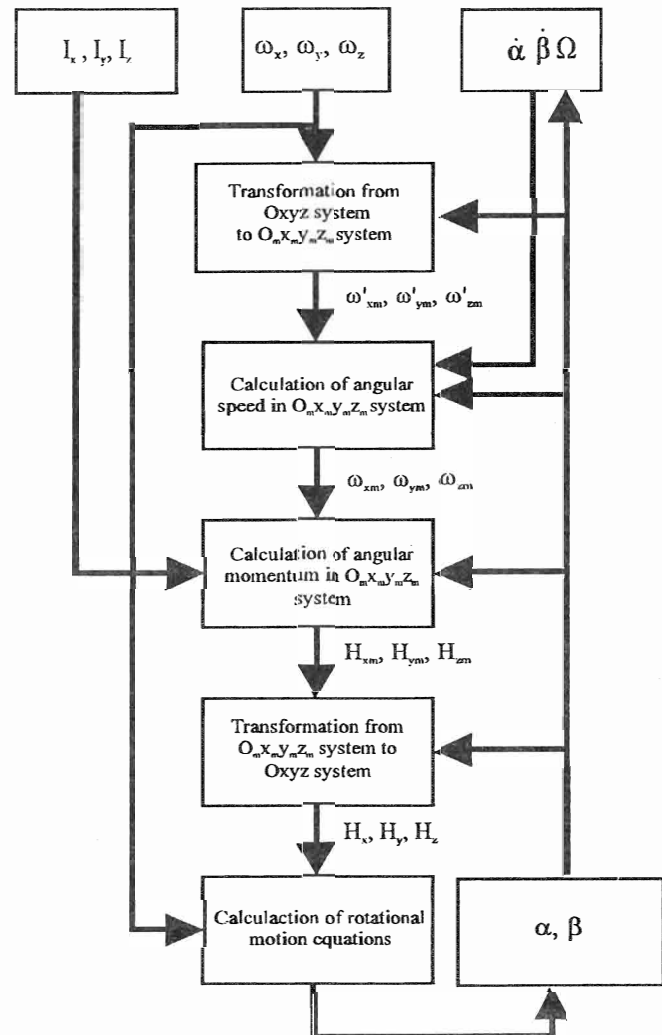


Fig. 2 Algorithm of calculation of left side of Euler's equations.

4 Rotational motion

The rotational motion in co-ordinate system Oxyz is described by Euler's equations [1]:

$$\begin{aligned} \frac{dH_x}{dt} + H_z \omega_y - H_y \omega_z &= M_x + M_{sz}, \\ \frac{dH_y}{dt} + H_x \omega_z - H_z \omega_x &= M_y + M_{sy}, \\ \frac{dH_z}{dt} + H_y \omega_x - H_x \omega_y &= M_z + M_{sz}, \end{aligned} \quad (5)$$

where: H_i - components of the angular momentum, ω_i - components of aircraft angular velocity, M_{si} - components of the resultant moment of forces connected with translational motion of the mass centre, M_i - components of the resultant moment of the external forces, which are:

$$\begin{aligned} M_x &= 0, \\ M_y &= F_{lz} \cdot l - F_{pz} \cdot p, \\ M_z &= F_{ly} \cdot l - F_{py} \cdot p. \end{aligned} \quad (6)$$

Forces: $F_{ly}, F_{py}, F_{lz}, F_{pz}$ - are described below of Eq. (4) and l, p - are distances between the left and right electromagnets, respectively and instrument geometric centre (by symmetry: $l = -p$).

The rotor moments of inertia are time functions in the coordinate system $Oxyz$ and they are constant in the coordinate system $O_m x_m y_m z_m$. Thus to calculate the components of angular momentum and next to derive the left side of Euler's equations the steps shown in Fig. 2 were undertaken. The resultant equations are as follows:

$$\begin{aligned} &(-\omega_y \dot{\alpha} \sin^2 \alpha \cos^2 \beta - \omega_z \dot{\beta} \cos \alpha \cos^2 \beta - \Omega \dot{\alpha} \sin \alpha \cos \beta + \dot{\alpha} \dot{\beta} \cos \alpha \sin^2 \beta + \omega_z \dot{\beta} \cos \alpha \sin^2 \beta - \dot{\alpha} \dot{\beta} \cos \alpha \cos^2 \beta + \omega_y \omega_z \sin^2 \alpha \cos^2 \alpha \cos^2 \beta + \dot{\omega}_x \cos^2 \alpha \cos^2 \beta + \dot{\beta} + \omega_z \dot{\alpha} \sin \alpha \sin \beta \cos \beta + \dot{\alpha}^2 \sin \alpha \sin \beta \cos \beta - 2 \omega_x \dot{\alpha} \sin \alpha \cos^2 \beta \cos \alpha - \dot{\omega}_z \cos \alpha \sin \beta \cos \beta - \omega_y^2 \cos \beta \sin \alpha \sin \beta - \omega_x \omega_y \cos \beta \cos \alpha \sin \beta + \sin \alpha \sin \beta \cos \beta \omega_z^2 - \ddot{\alpha} \cos \alpha \sin \beta \cos \beta - 2 \omega_x \dot{\beta} \cos^2 \alpha \sin \beta \cos \beta + \dot{\alpha} \omega_z \sin \alpha \sin \beta \cos \beta + \dot{\alpha} \omega_y \sin^2 \beta - 2 \omega_y \dot{\beta} \cos \alpha \sin \beta \sin \alpha \cos \beta - \Omega \dot{\beta} \cos \alpha \sin \beta - \Omega \omega_y \sin \beta + \dot{\omega}_y \cos \alpha \cos \beta \sin \alpha - \omega_y \omega_z \sin^2 \alpha \cos^2 \beta - \Omega \omega_z \sin \alpha \cos \beta - \omega_x \omega_z \sin \alpha \cos^2 \beta \cos \alpha) I_x + (\omega_y \dot{\alpha} \sin^2 \alpha - \omega_y \dot{\alpha} \cos^2 \alpha - \dot{\beta} \sin \alpha + 2 \omega_x \dot{\alpha} \cos \alpha \sin \alpha + \dot{\omega}_x \sin^2 \alpha - \dot{\omega}_y \sin \alpha \cos \alpha - \dot{\alpha} \dot{\beta} \cos \alpha + \omega_x \omega_z \cos \alpha \sin \alpha - \omega_y \omega_z \cos^2 \alpha - \dot{\beta} \omega_z \cos \alpha) I_y + (\omega_z \dot{\beta} \cos \alpha \cos^2 \beta + \dot{\omega}_x \cos^2 \alpha \sin^2 \beta + \dot{\omega}_z \cos \alpha \sin \beta \cos \beta + \dot{\omega}_y \cos \alpha \sin^2 \beta \sin \alpha - \dot{\alpha} \dot{\beta} \cos \alpha \sin^2 \beta + \omega_y^2 \cos \beta \sin \alpha \sin \beta + \omega_y \dot{\alpha} \cos^2 \alpha \sin^2 \beta - \omega_z \dot{\beta} \cos \alpha \sin^2 \beta - \omega_y \dot{\alpha} \sin^2 \alpha \sin^2 \beta + \omega_y \omega_z \cos^2 \beta + \omega_y \dot{\alpha} \cos^2 \beta + \dot{\alpha} \dot{\beta} \cos \alpha \cos^2 \beta + \omega_x \omega_y \cos \beta \cos \alpha \sin \beta - 2 \omega_x \dot{\alpha} \sin \alpha \sin^2 \beta \cos \alpha - \omega_z^2 \sin \alpha \sin \beta \cos \beta - \omega_z \dot{\alpha} \sin \alpha \sin \beta \cos \beta - \dot{\alpha}^2 \sin \alpha \sin \beta \cos \beta + \ddot{\alpha} \cos \alpha \sin \beta \cos \beta + 2 \omega_x \dot{\beta} \cos^2 \alpha \sin \beta \cos \beta + 2 \omega_y \dot{\beta} \cos \alpha \sin \beta \sin \alpha \cos \beta - \omega_x \omega_z \sin \alpha \sin^2 \beta \cos \alpha - \omega_y \omega_z \sin^2 \alpha \sin^2 \beta - \omega_z \dot{\alpha} \sin \alpha \sin \beta \cos \beta) I_z = M_x - m(a_x y - a_y x), \end{aligned} \quad (7a)$$

$$\begin{aligned} &(-\dot{\alpha} \dot{\beta} \sin \alpha \cos^2 \beta + \Omega \dot{\alpha} \cos \alpha \cos \beta + \omega_x \dot{\alpha} \cos^2 \alpha \cos^2 \beta + \omega_z \dot{\beta} \sin \alpha \sin^2 \beta - \dot{\alpha}^2 \cos \alpha \cos \beta \sin \beta + 2 \omega_y \dot{\alpha} \cos \alpha \cos^2 \beta \sin \alpha - \omega_z \dot{\alpha} \cos \alpha \cos \beta \sin \beta + \dot{\alpha} \dot{\beta} \sin \alpha \sin^2 \beta - \omega_x \dot{\alpha} \sin^2 \alpha \cos^2 \beta + \Omega \omega_x \sin \beta + \dot{\omega}_y \sin^2 \alpha \cos^2 \beta - \omega_x \dot{\alpha} \sin^2 \beta - \Omega \dot{\beta} \sin \alpha \sin \beta - \omega_x \omega_z \sin^2 \beta - \ddot{\alpha} \sin \alpha \sin \beta \cos \beta - \omega_z \dot{\alpha} \cos \alpha \sin \beta \cos \beta - \omega_z \sin \alpha \cos^2 \beta - 2 \omega_x \dot{\beta} \sin \alpha \sin \beta \cos \alpha \cos \beta - \omega_z^2 \cos \alpha \sin \beta \cos \beta - 2 \omega_y \dot{\beta} \sin^2 \alpha \sin \beta \cos \beta - \sin \alpha \sin \beta \cos \beta \dot{\omega}_z + \omega_x^2 \cos \beta \cos \alpha \sin \beta + \dot{\omega}_x \sin \alpha + \omega_x \omega_y \cos \beta \sin \alpha \sin \beta \cos^2 \beta \cos \alpha + \omega_x \omega_z \cos^2 \alpha \cos^2 \beta + \omega_z \Omega \cos \alpha \cos \beta + \omega_y \omega_z \cos \alpha \cos^2 \beta \sin \alpha) I_x + (\ddot{\alpha} \sin \alpha \sin \beta \cos \beta + \omega_z \dot{\alpha} \cos \alpha \sin \beta \cos \beta + \omega_z \dot{\beta} \sin \alpha \cos^2 \beta + \dot{\alpha} \dot{\beta} \sin \alpha \cos^2 \beta + \omega_y \omega_z \cos \alpha \sin^2 \beta \sin \alpha + \dot{\omega}_y \sin^2 \alpha \sin^2 \beta - \omega_x \dot{\alpha} \sin^2 \alpha \sin^2 \beta + \omega_x \omega_z \cos^2 \alpha \sin^2 \beta + 2 \omega_x \dot{\beta} \sin \alpha \sin \beta \cos \alpha \cos \beta + 2 \omega_y \dot{\beta} \sin^2 \alpha \sin \beta \cos \beta - \omega_z \dot{\beta} \sin \alpha \sin^2 \beta + \omega_z^2 \cos \alpha \sin \beta \cos \beta + \dot{\omega}_x \sin \alpha \sin^2 \beta \cos \alpha + \dot{\omega}_z \sin \alpha \sin \beta \cos \beta + \omega_x \dot{\alpha} \cos^2 \alpha \sin^2 \beta - \dot{\alpha} \dot{\beta} \sin \alpha \sin^2 \beta + \omega_z \dot{\alpha} \cos \alpha \cos \beta \sin \beta + \dot{\alpha}^2 \cos \alpha \cos \beta \sin \beta - \omega_x^2 \cos \beta \cos \alpha \sin \beta + 2 \omega_y \dot{\alpha} \cos \alpha \sin^2 \beta \sin \alpha - \omega_x \omega_y \cos \beta \sin \alpha \sin \beta - \omega_x \omega_z \cos^2 \beta - \omega_x \dot{\alpha} \cos^2 \beta) I_z + (-\omega_x \dot{\alpha} \cos^2 \alpha + \dot{\omega}_x \cos^2 \alpha + \dot{\beta} \cos \alpha + \omega_x \dot{\alpha} \sin^2 \alpha - \dot{\alpha} \dot{\beta} \sin \alpha - \cos \alpha \sin \alpha \dot{\omega}_x + \omega_x \omega_z \sin^2 \alpha - \omega_y \omega_z \sin \alpha \cos \alpha - \omega_z \dot{\beta} \sin \alpha - 2 \omega_y \dot{\alpha} \sin \alpha \cos \alpha) I_y = M_y - m(a_x z - a_z x) - F_x z, \end{aligned} \quad (7b)$$

$$\begin{aligned} &(-\Omega \dot{\beta} \cos \beta + \ddot{\alpha} \sin^2 \beta + \dot{\omega}_x \sin^2 \beta + \omega_x \dot{\alpha} \cos \beta \sin \alpha \sin \beta + \omega_x \dot{\beta} \sin^2 \beta \cos \alpha + \omega_y \dot{\beta} \sin^2 \beta \sin \alpha + \omega_x^2 \sin \alpha \cos^2 \beta \cos \alpha + \omega_x \omega_y \sin^2 \alpha \cos^2 \beta + \Omega \omega_x \sin \alpha \cos \beta + \omega_y \omega_z \cos \alpha \sin \beta \cos \beta + \omega_y \dot{\alpha} \cos \alpha \sin \beta \cos \beta - \omega_y \dot{\alpha} \cos \beta \cos \alpha \sin \beta - \omega_x \dot{\beta} \cos^2 \beta \cos \alpha - \omega_y \dot{\beta} \cos^2 \beta \sin \alpha + 2 \omega_z \dot{\beta} \cos \beta \sin \beta + 2 \dot{\alpha} \dot{\beta} \cos \beta \sin \beta - \dot{\omega}_x \cos \beta \cos \alpha \sin \beta - \dot{\omega}_y \cos \beta \sin \alpha \sin \beta - \omega_x \omega_z \sin \alpha \sin \beta \cos \beta - \omega_x \dot{\alpha} \sin \alpha \sin \beta \cos \beta - \cos \alpha \cos^2 \beta \sin \alpha \omega_y^2 - \omega_x \omega_y \cos^2 \alpha \cos^2 \beta - \omega_y \Omega \cos \alpha \cos \beta) I_x + (\omega_x \omega_y \cos^2 \alpha - \omega_x^2 \cos \alpha \sin \alpha + \omega_x \dot{\beta} \cos \alpha + \omega_y^2 \sin \alpha \cos \alpha - \omega_x \omega_y \sin^2 \alpha + \omega_y \dot{\beta} \sin \alpha) I_y + (-2 \dot{\alpha} \dot{\beta} \cos \beta \sin \beta + \omega_x \omega_z \sin \alpha \sin \beta \cos \beta + \omega_x \dot{\alpha} \sin \alpha \sin \beta \cos \beta + \omega_x^2 \sin \alpha \sin^2 \beta \cos \alpha + \omega_x \omega_y \sin^2 \alpha \sin^2 \beta - \omega_x \dot{\beta} \sin^2 \beta \cos \alpha - \omega_y \dot{\beta} \sin^2 \beta \sin \alpha + \omega_y \dot{\alpha} \cos \beta \cos \alpha \sin \beta - \omega_x \dot{\alpha} \cos \beta \sin \alpha \sin \beta + \omega_y \dot{\beta} \cos^2 \beta \sin \alpha + \dot{\omega}_x \cos \beta \cos \alpha \sin \beta - 2 \omega_z \dot{\beta} \cos \beta \sin \beta + \ddot{\alpha} \cos^2 \beta + \omega_x \dot{\beta} \cos^2 \beta \cos \alpha + \dot{\omega}_x \cos^2 \beta - \omega_x \omega_y \cos^2 \alpha \sin^2 \beta - \omega_y^2 \cos \alpha \sin^2 \beta \sin \alpha + \dot{\omega}_y \cos \beta \sin \alpha \sin \beta - \omega_y \dot{\alpha} \cos \alpha \sin \beta \cos \beta - \omega_y \omega_z \cos \alpha \sin \beta \cos \beta) I_z = M_z - m(a_y x - a_x y) + F_x y. \end{aligned} \quad (7b)$$

Eqs 4 and 7 are a set of exact full equations describing the rotor motion. To obtain the simplified linear equations we introduce the following assumptions.

1. Shift of the inertial mass centre O_m from the instrument geometric centre O is very small. By this assumption we can uncouple the translational motion and rotational motion of the inertial mass.
2. Angles α , β between frame of references: $Oxyz$, $O_mx_my_mz_m$ are small. Thus: $\sin\alpha \approx \alpha$, $\sin\beta \approx \beta$, $\cos\alpha \approx 1$, $\cos\beta \approx 1$.
3. Angular speed of the rotor rotation Ω is much faster than other angular speeds under consideration. Thus, the components of angular momentum in direction of axes: y_m , z_m are much smaller than component in direction of axis x_m .

The equations of rotational motion reduce to the form:

$$\begin{aligned} I_y \ddot{\alpha} + I_x \Omega \dot{\beta} + I_x \Omega \omega_x \alpha &= M_x - I_y \dot{\omega}_y - I_x \Omega \omega_z, \\ I_y \ddot{\beta} - I_x \Omega \dot{\alpha} + I_x \Omega \omega_x \beta &= M_y - I_y \dot{\omega}_z + I_x \Omega \omega_y. \end{aligned} \quad (8)$$

Eqs (4) and (8) are a set of five simplified differential equations describing the motion of inertial mass as a free body. Sixth degree of freedom is connected with rotational motion forced by electric motor.

5 Measurement path

Let the inertial mass is forced by electromagnets to move in such a way that the co-ordinate systems : $Oxyz$, $O_mx_my_mz_m$ cover each other. Then (from (4) and (8)):

$$\begin{aligned} F_{ex} + mg_x - ma_{ox} &= 0, \\ F_{ey} + mg_y - ma_{oy} + F_{sy} &= 0, \\ F_{ez} + mg_z - ma_{oz} + F_{sz} &= 0, \\ M_x - I_y \dot{\omega}_y - I_x \Omega \omega_z &= 0, \\ M_y - I_y \dot{\omega}_z + I_x \Omega \omega_y &= 0. \end{aligned} \quad (9)$$

Acceleration a_{ox} can be calculated from the Eq. (9) if we are able to measure the force F_{ex} and when the gravity acceleration is known. As it is described in [4], force F_{ex} can be calculated from equation:

$$F_{ex} = k_{ix} i_x + k_x x, \quad (10)$$

where: k_{ix} - current stiffness, i_x - control current in the coil, k_x - displacement stiffness. In our case $x=0$ and measurement of control current is sufficient to calculate force F_{ex} , and thus to calculate the acceleration a_{ox} .

The last four equations in the set (9) are coupled by relations (6). The radial electromagnets generate forces which compensate as well the forces: \bar{F}_l , \bar{F}_p generated by translational motion as the forces: \bar{F}_l , \bar{F}_p generated by rotational motion. Indices: l , p refer to planes containing axes of the left and right radial electromagnets. Since the instrument is symmetric the forces are: $\bar{F}_l = \bar{F}_p = \bar{F}_l$ and $\bar{F}_l = -\bar{F}_p = \bar{F}_l$. The forces in left \bar{F}_{el} and right \bar{F}_{ep} electromagnets are as follows:

$$\begin{aligned} \bar{F}_{el} &= \bar{F}_l + \bar{F}_r, \\ \bar{F}_{ep} &= \bar{F}_l - \bar{F}_r. \end{aligned} \quad (11)$$

All these forces are complex vectors since for example $\bar{F}_{el} = F_{ly} + j \cdot F_{lz}$, $j = \sqrt{-1}$. The forces \bar{F}_l , \bar{F}_r can be calculated from above relations. \bar{F}_r is proportional to the angular speed but \bar{F}_l is contaminated by electromagnetic force generated by electric motor. Thus, the instrument can measure simultaneously the acceleration a_x in the axial direction, and angular speeds ω_y , ω_z . Therefore, to measure all variable of aircraft motion there are needed three such instruments on the board with mutually perpendicular axes of rotation.

6 System simulation

To check performance of the gyroscope its dynamics and measurement path were simulated in the MATLAB-SIMULINK environment. There are used two models of gyroscope dynamics: full and simplified. The control law is designed for simplified linear instrument model. Controller consists of observer and LQR regulator [3]. The same control law is joined to the full model and to the simplified one. Parameters of simulation are the same for two models, so we can compare the results of simulation immediately. In this case the detailed information due gyroscope model parameters and measurement path parameters is not so important.

The extreme excitations are joined to the gyroscope models to study the gyroscope behaviour in different situations. The excitations are in the form of step functions as follows.

1. Aircraft angular velocity ω_y was in 0.01s changed from $0^\circ/s$ up to $400^\circ/s$.
2. Aircraft angular velocity ω_z was in 0.02s changed from $0^\circ/s$ up to $400^\circ/s$.
3. Aircraft linear acceleration was in 0.03s changed simultaneously in the direction of all axes of $Oxyz$ system from $0g$ up to $20g$.

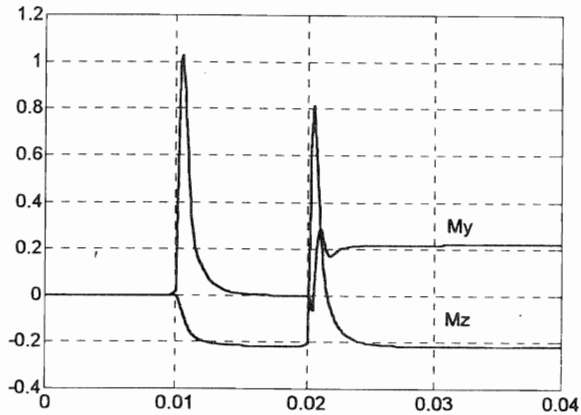
To avoid of the differentiation of step function the change of the value in step is a little stretched in time. Such situation is much more similar to the natural one, since angular velocity and linear acceleration step changes are not possible in aircraft performance.

Different signals in gyroscope models and measurement paths caused by above excitations were recorded and analysed. These signals are as follows.

1. Components M_y , M_z of resultant moment of external forces (gyrostatic moment) in measurement paths (denoted in Fig. 3 as: M_y , M_z).
2. Rotor displacement in bearing planes caused by angular velocity step functions (denoted in Figs 3, 6 as: yr , zr , $yr1$, $zr1$).

3. Rotor displacement in bearing planes caused by linear acceleration step function (denoted in Fig. 4 as: y_u, z_u).
4. Rotor mass centre displacement in direction of axis Ox caused by linear acceleration step function (Fig. 5).
5. Axial force F_x in measurement paths caused by linear acceleration step function (Fig. 5).

a)



b)

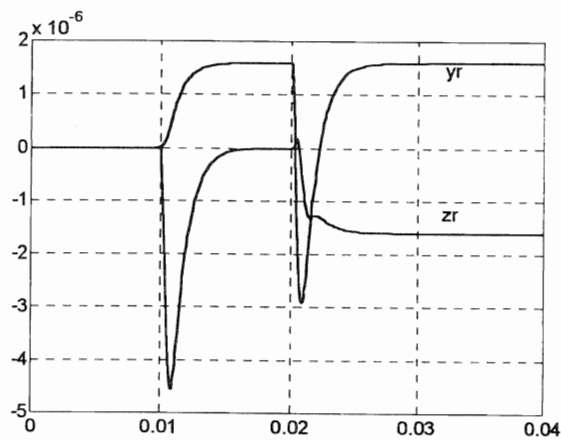


Fig.3. Full model answer to angular velocity step functions; a) measured gyrostatic moments, b) rotor displacement in bearing planes.

Index 1 in above notations refers to the simplified model. Figs 3-5 show time signals for full model. They conform the proper performance of the gyroscope with magnetically supported rotor

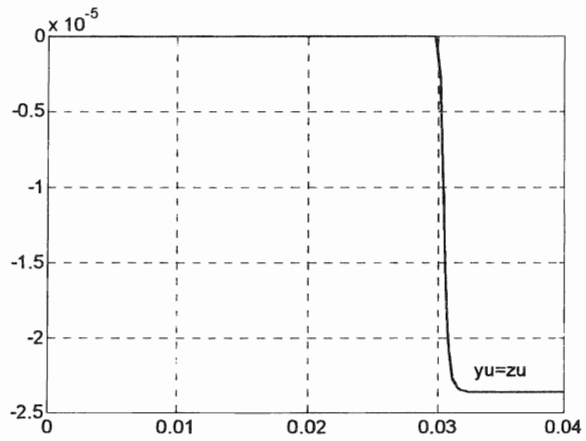
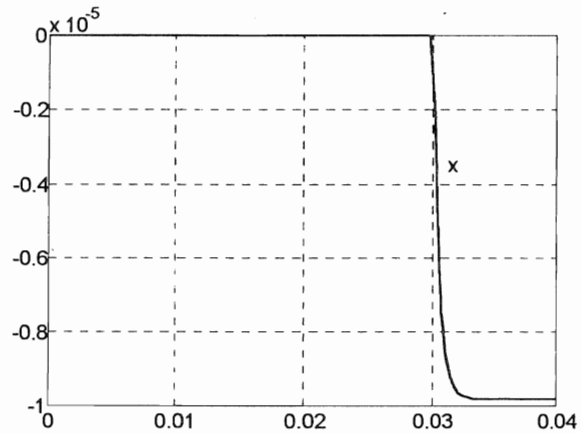


Fig.4. Rotor displacement in bearing planes as a response to linear acceleration step function.

a)



b)

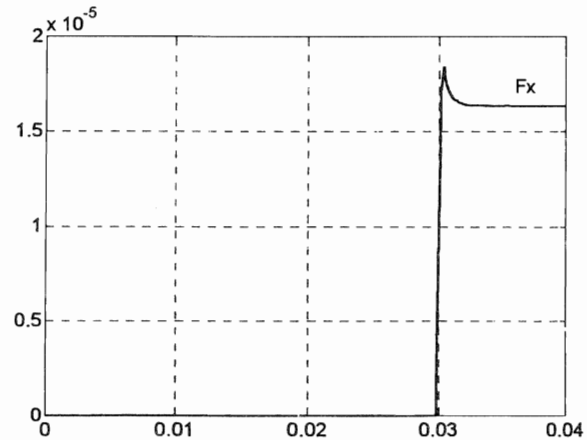


Fig.5. Full model answer to linear acceleration step function; a) axial displacement x of rotor mass centre, b) axial force F_x .

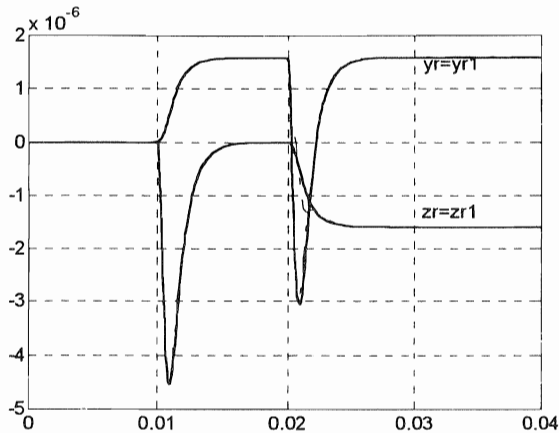


Fig. 6. Rotor displacements in bearing plane for full and simplified models which are the answer to angular velocity step functions.

As it is seen in Fig. 3 the model answer to the angular velocity ω_y and ω_z steps in 0.01 s and 0.02s, respectively is such as we expected. Angular velocity ω_y causes impulse of component M_y and steady-state value of M_z . Next, the component M_z causes steady-state of rotor displacement y_r and the component M_y generates a impulse of rotor displacement z_r . Similar cross relation are also right for excitation by angular velocity ω_z . It should be noted, that linear acceleration step function which was joined to the input in 0.03s did not cause any noticeable changes in above characteristics. It confirms that the translational and rotational motions can be decoupled.

Components a_{oy} , a_{oz} of linear acceleration step function, which was joined after 0.03s from the beginning of the simulation, generate the rotor displacements in bearing planes in the direction of the same axes: O_y , O_z , as it is shown in Fig. 4.

The rotor displacement and axial force in the direction of axis O_x are shown in Fig. 5. This measurement path can be used to calculate the linear acceleration of the aircraft in this direction. To do it we need additional information about component of gravity acceleration in this direction.

The components of rotor displacement in the bearing planes generated by angular velocity steps for full and simplified gyroscope model was shown in Fig. 6. We can see small differences in the same signals only for transient motion. For steady-state the difference is invisible since for example the signal $y_r = 0.16 \cdot 10^{-5}$ and signal $y_{r1} = 0.1593 \cdot 10^{-5}$ so the difference is of order $7 \cdot 10^{-9}$. Similar results were obtained for other time characteristics so they are not shown here.

7 Conclusions

The exact full equations of rotor motion in gyroscope with magnetic suspension were derived in the paper. These equations are nonlinear and nonstationary and the translational and rotational rotor motions are coupled. In INS gyroscope the rotor motion should follow the gyroscope

case motion. In our case this task is realised by control system of magnetic field. The control law was designed for simplified linear stationary model of gyroscope.

Two simulation models are made for gyroscope dynamics and its measurement path.

1. The control law was joined to full nonlinear, nonstationary gyroscope model. It is so called the full reference model.
2. The control law was joined to simplified linear gyroscope model. It allowed to estimate the influence of the simplification on the exactness of the measurement path.

Results of computer simulation indicate that the following simplifications are allowed.

1. Translational and rotational motion can be decoupled.
2. Additional moments of forces resulting from translational motion of rotor mass centre from instrument geometric centre are neglectfully small.
3. Simplified model can be used to design the control law and measurement path.

Nevertheless, the knowledge about simplification can be useful in corrections of gyroscope performance to minimise its drift as it takes place in the „classic” gyroscope with mechanically supported rotor.

References

- [1] Magnus K.: *Kreisel-Theorie und Anwendungen* Springer-Verlag Berlin 1971.
- [2] Schweitzer G., Traxler A., Bleuler H.: *Magnetlager*. Springer - Verlag, Berlin 1993.
- [3] Vischer D.: "Sensorlose und spannungsgesteuerte Magnetlager". Diss. ETH Nr. 8665, Zurich 1988.
- [4] Gosiewski Z., Grzegorzczak T., Falkowski K.: "Navigational Instruments with Magnetically Suspended Inertial Masses". *Proc. 6th Int. Symposium on Transport Phenomena and Dynamics of Rotating Machinery ISROMAC-6*, pp. 612-618, Honolulu 1996.
- [5] Gosiewski Z., Grzegorzczak T., Falkowski K.: "Przyrządy lotnicze z zawieszoną magnetycznie masą pomiarową - giroskop". *Materiały II Szkoły "Aktywne Metody Redukcji Drgan i Hałasu"*. str. 49-54, Zakopane 1995.